

# Kinematic and Mechanical Profile of the Self-Actuation of Thermosalient Crystal Twins of 1,2,4,5-Tetrabromobenzene: A Molecular Crystalline Analogue of a Bimetallic Strip

Subash Chandra Sahoo,<sup>†,‡</sup> Shashi Bhushan Sinha,<sup>‡,‡</sup> M. S. R. N. Kiran,<sup>§</sup> Upadrasta Ramamurty,<sup>§</sup> Arcan F. Dericioglu,<sup>||</sup> C. Malla Reddy,<sup>\*,‡</sup> and Panče Naumov<sup>\*,†</sup>

<sup>†</sup>New York University Abu Dhabi, P.O. Box 129188, Abu Dhabi, United Arab Emirates

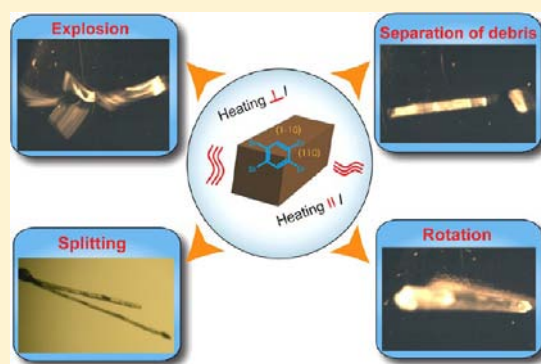
<sup>‡</sup>Indian Institute of Science Education and Research, Kolkata, West Bengal 741252, India

<sup>§</sup>Department of Materials Engineering, Indian Institute of Science, Bangalore 560012, India

<sup>||</sup>Department of Metallurgical and Materials Engineering, Middle East Technical University, 06800 Ankara, Turkey

## S Supporting Information

**ABSTRACT:** A paradigm shift from hard to flexible, organic-based optoelectronics requires fast and reversible mechanical response from actuating materials that are used for conversion of heat or light into mechanical motion. As the limits in the response times of polymer-based actuating materials are reached, which are inherent to the less-than-optimal coupling between the light/heat and mechanical energy in them, a conceptually new approach to mechanical actuation is required to leapfrog the performance of organic actuators. Herein, we explore single crystals of 1,2,4,5-tetrabromobenzene (TBB) as actuating elements and establish relations between their kinematic profile and mechanical properties. Centimeter-size acicular crystals of TBB are the only naturally twinned crystals out of about a dozen known materials that exhibit the *thermosalient effect*—an extremely rare and visually impressive crystal locomotion. When taken over a phase transition, crystals of this material store mechanical strain and are rapidly self-actuated to sudden jumps to release the internal strain, leaping up to several centimeters. To establish the structural basis for this colossal crystal motility, we investigated the mechanical profile of the crystals from macroscale, in response to externally induced deformation under microscope, to nanoscale, by using nanoindentation. Kinematic analysis based on high-speed recordings of over 200 twinned TBB crystals exposed to directional or nondirectional heating unraveled that the crystal locomotion is a kinematically complex phenomenon that includes at least six kinematic effects. The nanoscale tests confirm the highly elastic nature, with an elastic deformation recovery (60%) that is far superior to those of molecular crystals reported earlier. This property appears to be critical for accumulation of stress required for crystal jumping. Twinned crystals of TBB exposed to moderate directional heating behave as all-organic analogue of a bimetallic strip, where the lattice misfit between the two crystal components drives reversible deformation of the crystal.



## 1. INTRODUCTION

The design of new actuating materials which are capable of fast, reversible, and controllable mechanical motions in response to external stimuli (thermal, light, magnetic, or electric field) is at the frontier of the contemporary materials science research.<sup>1–7</sup> The research efforts in this field are driven by the potentials for utility of such motions to perform mechanical work in bulk materials, which could have far-reaching technological implications as mechanically active elements. Most of the current macroscopic artificial actuators are fabricated from thermo- or photoactive elastomeric or liquid-crystalline materials.<sup>8–23</sup> Although the mechanically responsive polymers have set the path to mechanical elements such as microfluidic valves and gates,<sup>24,25</sup> mechanooptoelectronics<sup>26–28</sup> and artificial muscles,<sup>29,30</sup> the future applications place extensive require-

ments to the performance of such materials, primarily fast or ultrafast energy transfer and resistance to fatigue.

The dense and ordered packing of single crystals is an underexploited platform for fast and efficient conversion of light or thermal energy into mechanical work. Traditionally, the potential for utility of single crystals as actuators to overcome these drawbacks has been contrasted by their generally poorer (relative to polymers) mechanical robustness. Indeed, there are only a handful of examples of photomechanical and thermomechanical effects where the integrity of single crystals is retained. The quest for efficient energy conversion and the advent of crystal engineering, however, have brought up

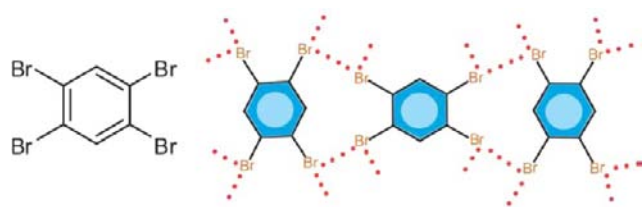
Received: June 12, 2013

Published: July 11, 2013

increasing evidence that contradicts the classical perception of single crystals as stiff entities. Indeed, under certain conditions single crystals of even extremely simple organic compounds can respond mechanically to light or external force with impressive elastic properties, thus setting the basis to engineer a new class of actuating materials.<sup>31–50</sup> Among the greatest assets of molecular single crystals for efficient photomechanical actuators are their advantageous elastic moduli that translate into strong actuating forces at small deformations. Indeed, although smaller absolute deformations can be expected relative to elastomers, certain single crystals are endowed with structures that can sustain larger local internal stresses.

Aimed at a quantitative assessment of the potential of organic crystals for macroscopic actuation, for this study we selected 1,2,4,5-tetrabromobenzene (TBB, Scheme 1). This simple,

**Scheme 1. Structure and Br⋯Br Interactions in Polymorph  $\beta$  of 1,2,4,5-Tetrabromobenzene (TBB)**



highly symmetrical molecule crystallizes readily as long, colorless, twinned crystals (>95% yield twins) that can reach dimensions of >2 cm and are twinned over the (110) mirror plane and elongated about their [001] axis. The crystals undergo structural phase transition between the room-temperature phase ( $\beta$ ), stable at ambient conditions, and a high-temperature phase ( $\gamma$ ) that is stable above 46 °C.<sup>51–55</sup> The transition is accompanied by a *thermosalient* (TS) effect,<sup>56–65</sup> an

impressive reversible mechanical response whereby crystals rapidly jump up to several centimeters high! Davey et al.<sup>51</sup> have attempted to disentangle the interplay between the intermolecular interactions, twinning, polymorphism and the phase transformation underlying this impressive motility. Although they have put forward a viable hypothesis of the important role of the weak Br⋯Br interactions in the mechanical response, the correlation between the mechanical response and the underlying structure has not been firmly established yet. In general, due to the limited number of reported materials that display the TS phenomenon, the effect has not received the necessary research attention in the past much beyond the occasional notion that certain crystals hop when heated or cooled.

Herein, we set as our goal to provide a detailed analysis and to unravel the nature of the driving force behind the impressive self-actuation of TBB crystals. We hypothesized that quantification of the mechanical response through kinematic assessment of the structure–mechanical property relationships could provide a basis for deeper understating of the phenomenon. To that end, we employed a synergy of microscopic kinematic analysis and mechanical characterization, both at macroscale and at nanoscale, to provide the most direct evidence of the reasons behind the mechanical response. The results point to the important role of the elastic mechanical properties at the nanoscale in these crystals. The elasticity is related to accumulation of sufficient latent strain that is required to fuel crystal motility.

## 2. RESULTS AND DISCUSSION

**2.1. Crystallization and phase transition.** Crystals of TBB were obtained by recrystallization of the commercially available compound from a xylene/acetone (1:1) mixture or by double recrystallization from a saturated toluene solution. After a number of screenings, we found that the largest crystals of TBB are obtained by incubation of saturated toluene solution at

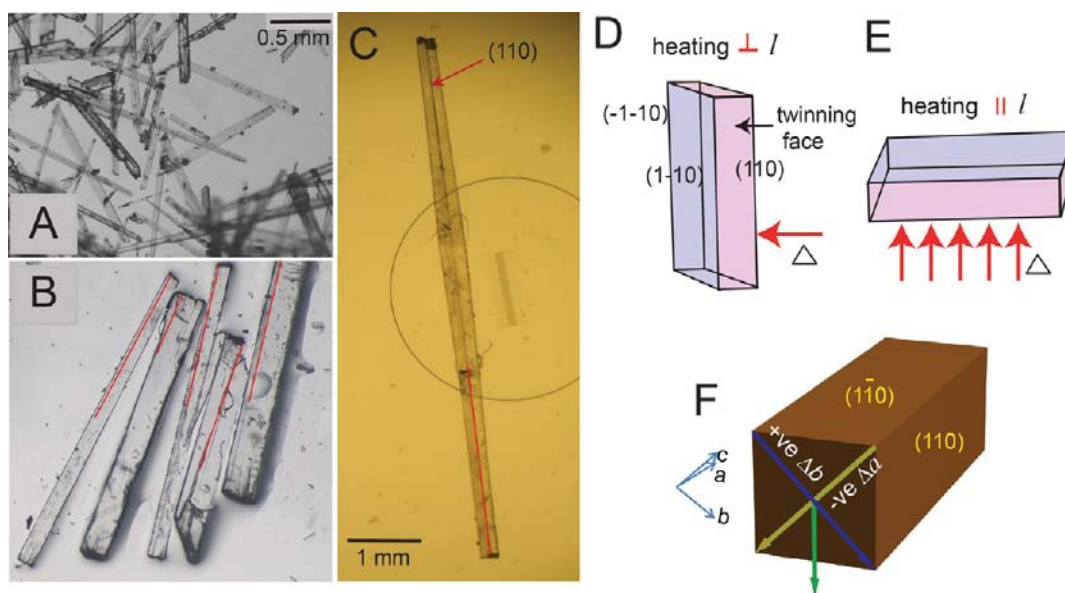


**Figure 1.** Appearance and twinning in the crystals of 1,2,4,5-tetrabromobenzene (TBB), and modes of heating used in the experiments. (A) General appearance of TBB crystals. (B) A group of twinned crystals having different size of their components. (C) Large twinned crystal having similar size of the two component crystals (the length of the linear scale is 1 mm). The twinning plane (110) is marked with a red line. (D) and (E) Schematic of the two heating modes, parallel (||) and perpendicular ( $\perp$ ), to the crystal length ( $l$ ) used in the kinematic analysis of the TBB crystals. (F) Macroscopic distortion of the crystal during the jumping (the green arrow shows the direction of the vector of the net momentum that propels the crystal off the stage).

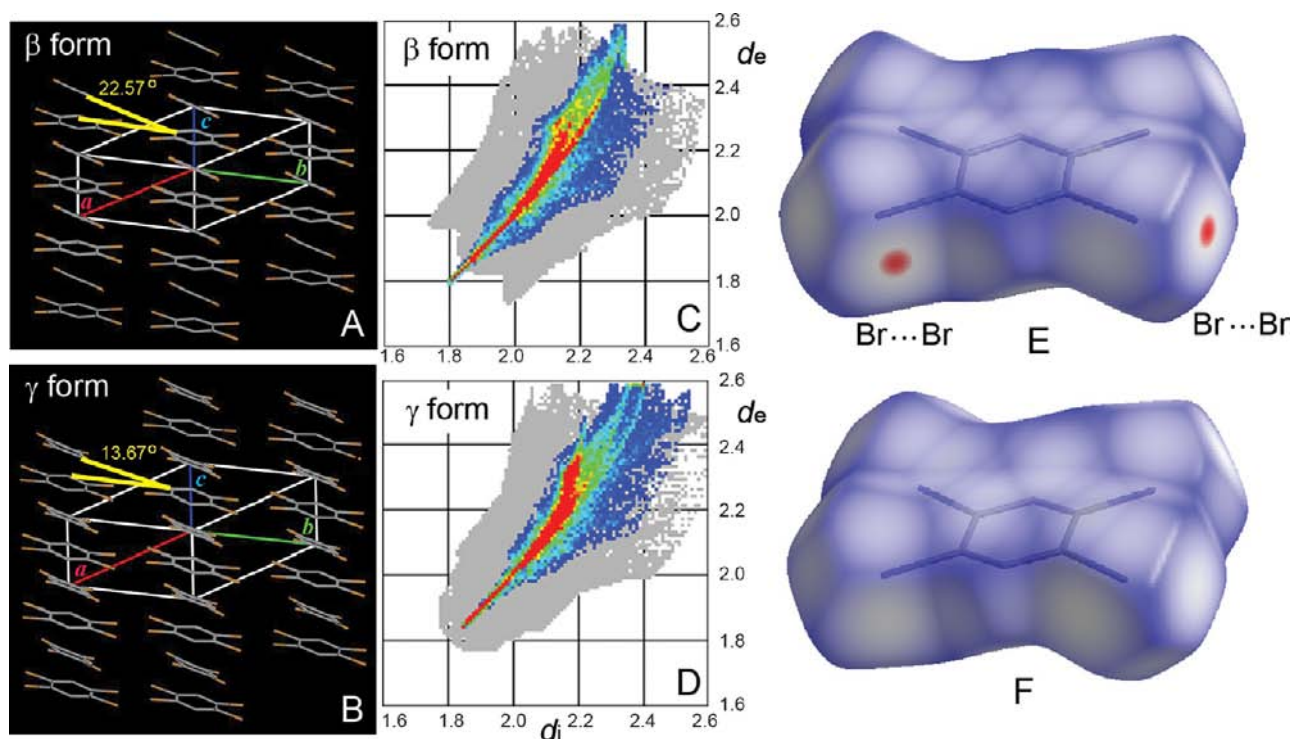


**Figure 2.** Crystal structures of the two forms of TBB,  $\beta$  and  $\gamma$  (A and B), and the respective Hirshfeld plots (C and D) and surfaces (E and F).

60 °C. Long twinned colorless crystals measuring between several millimeters and >2 cm in length were harvested after 24 h (Figure 1A). Inspection under polarized light showed that over 95% of the crystals were twinned and elongated about [001] (Figure 1B). The two components of the twin rarely had the same thickness, and usually one of the components was markedly thicker than the other. Comparison of the cell parameters (Table S1 in Supporting Information [SI]) with those from the earlier crystal structure determinations<sup>51–53</sup> confirmed that all crystals were of the  $\beta$  phase.

When heated on a hot plate, the crystals underwent structural phase transition between form  $\beta$ , stable at room temperature, and form  $\gamma$  which is stable above 46 °C. In the course of the transition some crystals jumped as high as several centimeters, while most of the smaller crystals flew off sideways (see movies si\_002.avi and si\_003.avi in the SI). The crystal jumps were also observed during cooling and upon second heating. The smaller amount of single crystals that were obtained in the crystallization experiments and were separated by hand also jumped in line with the fact that the effect is not solely a result of the twinning.

## 2.2. Structural Changes during the Phase Transition.

To unravel the reasons behind the impressive mechanical response, the structures of the two polymorphs were analyzed. As expected from the high rigidity of the TBB molecule, the comparison of the two structures shows absence of conformational changes within the individual molecules. In line with previous observations,<sup>51</sup> the phase transition from  $\beta$  to  $\gamma$  is accompanied by small changes in the cell parameters ( $\Delta a = -0.323$ ,  $\Delta b = 0.475$ ,  $\Delta c = 0.052$  Å,  $\Delta\beta = 1.44^\circ$ ,  $\Delta V = 8.163$  Å<sup>3</sup>). The cell of the  $\gamma$  phase expands 4.44% along the  $b$  axis and contracts 3.13% along the  $a$  axis. Notably, the change is negligible along the  $c$  axis, which coincides with the longest dimension of the crystal. It should be noted that the primary faces, (100) and (010), are absent in the crystal morphology;

the pairs of two side faces are (110)/( $\bar{1}\bar{1}0$ ) and ( $1\bar{1}0$ )/( $\bar{1}10$ ). Hence the vector of contraction and expansion of the  $a$  and  $b$  axes, respectively, has to be considered to understand the impact the face of a crystal makes on the hot-plate surface at the time of jumping on phase transformation. Here this vector is nearly perpendicular to the pair of major faces, ( $1\bar{1}0$ )/( $\bar{1}10$ ). This means that, at least in cases where the crystal remains intact during the jumping, the effective change in its shape prompts it to push off the surface, and the counterforce results in the jumping effect. A close observation of the crystal packing along the [001] direction suggests that the packing motifs of the two polymorphs are very similar with only minor difference in orientation of the unit cell (A and B of Figure 2). Although the slight difference in the packing viewed from the other directions is easier to inspect, the structural differences between the two polymorphs are miniscule.

The flat molecules are assembled into alternating layers of weak Br...Br and Br...H interactions (Scheme 1). Comparison of the packing of the two phases indicates that the thermal strain builds up on heating and transfers throughout the crystal by slight twisting of the substituted benzene ring within the plane. We quantified this change by measuring the angle between the planes of two distinctly oriented molecules from adjacent stacked columns (A and B of Figure 2). The molecules in the alternate columns twist only about 8.9° in accordance with the low enthalpy of the phase transition (0.315 kJ mol<sup>-1</sup>).<sup>51</sup> Since the phase transformation is devoid of other molecular movements, the overall macroscopic differences must arise from this collective, but sudden twisting motion. The small magnitude of the molecular perturbation (tilt of 8.9°) and the similarity of the two structures account for the reversibility of the phase transition on cooling.

The conformity between the environment of the TBB molecule in the two phases was additionally examined from the plots of the respective Hirshfeld surfaces (C–F of Figure

2).<sup>66–70</sup> The differences in the Hirshfeld fingerprint images for the two structures are readily distinguishable, indicating different molecular environments in the two structures. The small changes in the plots are due to different Br⋯Br distances (3.619 Å in the  $\beta$  form as compared to 3.729 Å in the  $\gamma$  form).

### 2.3. Quantification of the Mechanical Properties.

Qualitative mechanical deformation tests performed by application of a mechanical stress using a pair of forceps and a metal needle while viewing the crystals under stereomicroscope confirmed that both  $\beta$  and  $\gamma$  polymorphs are brittle and break when stressed (Figure S1, SI). This suggests that the weak  $\pi$ -stacking interaction planes between the corrugated layers in both forms do act as cleavage planes and not as slip planes.<sup>31</sup> The similarity in mechanical properties is expected from the similarity of the crystal structures of the two forms.

The nanoindentation technique has proven useful to establish a reliable structure/mechanical property correlation in molecular crystals by quantifying their mechanical properties, i.e. reduced elastic modulus ( $E_r$ ) and hardness ( $H$ ), of different crystal faces.<sup>71</sup> In the present study we obtained the indentation data from the  $(1\bar{1}0)$  face of the low-temperature  $\beta$  form of TBB (Figure 3; indentation could not be accomplished for  $\gamma$ -TBB

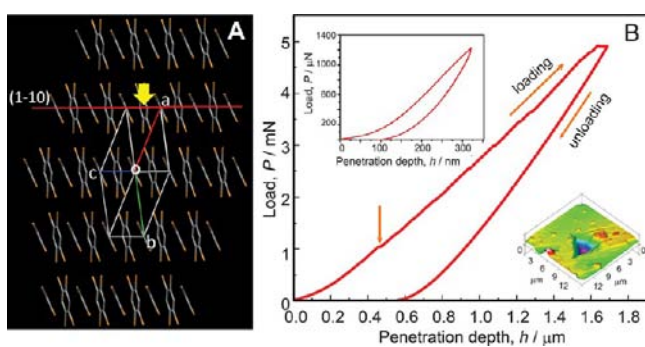


**Figure 3.** (A) Crystal packing of the  $\beta$  form showing the orientation of molecules with respect to the indentation direction. (B) Representative  $P$ – $h$  (load–displacement) curve obtained by nanoindentation on the  $(1\bar{1}0)$  of the  $\beta$  form. The insets in panel B show a 3D image of the indent impression (bottom right) and the  $P$ – $h$  curve of another indent with larger elastic recovery at lower peak force ( $\sim 1.3$  mN) (top left).

because our setup operated at ambient temperature). This face corresponds to the molecular arrangement where the difference between the two polymorphs was discernible, while the other faces were small and thus they were not suitable for indentation (Figure 3A). Although a small difference in structure could lead to a considerable change in mechanical properties, since the qualitative tests indicated similar mechanical behavior, we anticipate comparable  $E_r$  and  $H$  values for both phases. Moreover, the mechanical properties, when measured at different experiment temperatures, cannot be directly compared because  $E_r$  and  $H$  vary with the temperature.

Figure 3 shows representative load vs displacement ( $P$ – $h$ ) curves and indent impressions on the crystal face. The  $P$ – $h$  curve shows small residual depths after completion of the loading–unloading cycle, which implies that significant elastic recovery occurs during unloading. Postindentation imaging of the indent does not show any pile-up along the indentation edges (see the inset in the bottom right of Figure 3B). The absence of pile-up implies that the plastic flow constitutes only

a small part of the total deformation, and confirms that the  $P$ – $h$  response is dominated by the elastic contribution. The average values of the  $H$  and  $E_r$ , extracted from the  $P$ – $h$  responses are  $672 \pm 9$  MPa and  $6414 \pm 124$  MPa, respectively. In line with this, the large elastic recovery ( $\sim 60\%$ ) is much higher than the elastic recovery for (100) of saccharin (9%),<sup>72</sup> (100) of aspirin (35%),<sup>73</sup> and (101) of sodium saccharinate (25%).<sup>74</sup> During indentation, molecules either stretch apart (elastic deformation) or slide relative to each other (plastic deformation).<sup>75</sup> This also suggests that the TBB molecules in the structure can tolerate local molecular movements and can regain their original positions upon release of the stress, without leaving much strain in the crystal. The absence of slip planes is also consistent with the conclusions from the nanoindentation experiments that the TBB molecules are prone to elastic rather than to plastic deformation.

**2.4. Kinematic Analysis.** To perform kinematic (motion) analysis, well-shaped, as-crystallized needle crystals of TBB were selected and heated in two different modes, parallel to the longest crystal axis ( $\parallel l$ ), using a hot plate (Figure 1E), and perpendicular to the longest crystal axis ( $\perp l$ ) by using a pointy heating element (Figure 1D). To record the trajectories in mode  $\parallel l$ , each needle crystal was placed on a hot plate and individually heated starting from room temperature until it jumped, around 46–48 °C. The crystals exhibited visually impressive locomotion, hopping in different directions and traveling several centimeters from their original position (see movies si\_002.avi and si\_003.avi in the SI). Because the rapid motion of the crystals could not be captured with ordinary camera (resolution: 30 s<sup>−1</sup>), we turned to a high-speed camera with time resolution of up to 10<sup>4</sup> s<sup>−1</sup> that enabled us to inspect fine details and to track the crystal motion. A total of 150 crystals were individually heated and examined.

The high-speed recordings showed that the crystal-hopping phenomenon is not kinematically uniform. Instead, a careful analysis of the crystal trajectories unraveled that the motility was due to at least six different kinematic effects. Movies si\_002.avi–si\_016.avi in the SI contain typical recordings, and Figure 4 shows snapshots of these characteristic kinematic effects. Notably, we observed a period of latency from the onset of heating until the motion occurred during which the crystals remained still. This latent period is probably related to insufficient and/or inhomogeneous heating, and is required for accrual of sufficient internal strain for actuation. The latent period was followed by a sudden and forceful jump. The crystals that jumped remained clear and transparent after the displacement. On cooling, they underwent the reverse phase transition and the jumping reoccurred.

The histograms in Figures 5 and 6 represent distribution of the relative number of crystals undergoing a particular kinematic effect over the crystal size (to account for the natural size distribution of the crystals, the number of crystals in a particular size range undergoing that effect was divided by the total number of crystals in the same size range). Analysis of the recordings clearly showed that the most common effects responsible for the actuation of the TBB crystals were separation of debris from the crystal (effect-1), rotation (effect-2), and splitting of the crystal followed by jumping (effect-3). The other four effects described in Figure 5 were much less frequent. Moreover, the type of mechanical effect depended on the average crystal length ( $l$ ), width ( $w$ ), thickness ( $t$ ), and volume ( $V_{cr}$ ).

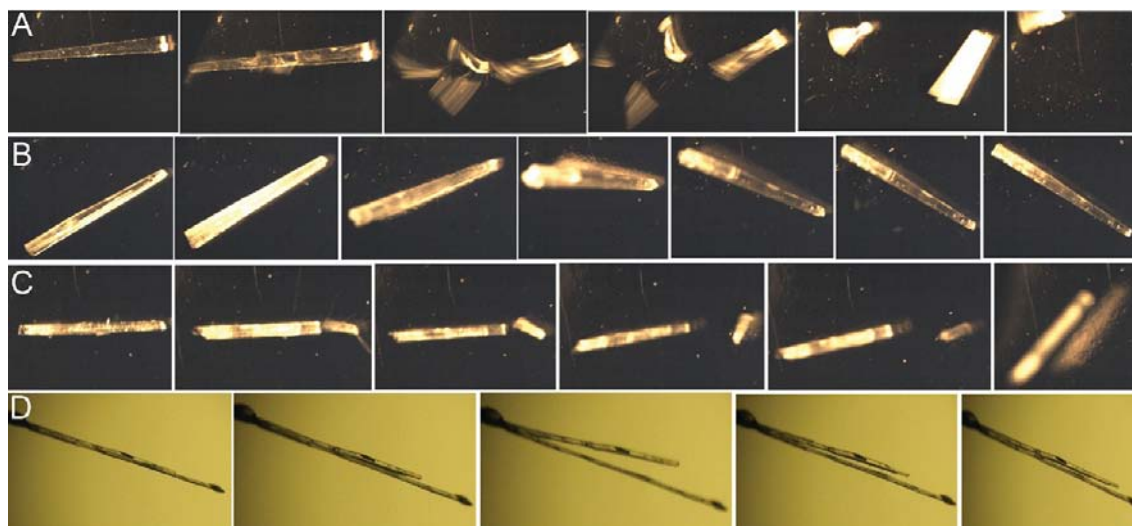


**Figure 4.** Series of snapshots showing different kinematic effects of thermal induced crystals of TBB: Splitting of crystal into several pieces with explosion (A), rolling or flipping of the crystal (B), separation of a small piece from the crystal that propels the remaining part into a spinning or linear motion (C), scissor-type motion of the two components of a split twin due to localized heating around the crystal (D). Typical recordings of these effects can be viewed in the SI (files si\_002.avi–si\_016.avi).

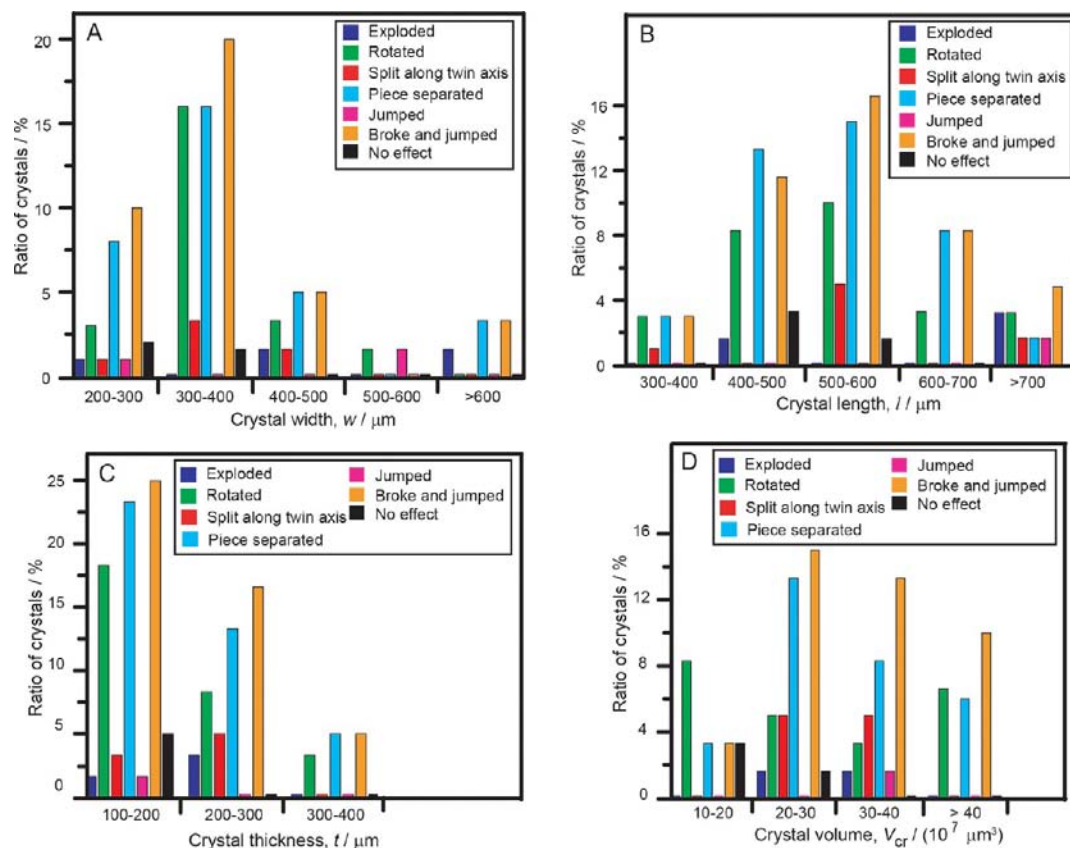


**Figure 5.** Distribution of the relative number of crystals over the kinematic effects for crystals heated uniformly and parallel ( $\parallel$ ) to the longest axis. The number of crystals in a particular size range undergoing a particular effect was divided by the total number of crystals in the same range.

For the heating mode  $\perp l$  (Figure 6), we observed maxima in the size distribution of these three kinematic effects with respect to all three dimensions ( $l$ ,  $w$ ,  $t$ ) and the volume ( $V_{cr}$ ) of the crystals. This result unravels, for the first time and on a statistically significant sample, the relation between the macroscopic properties of the thermosolient crystals and the kinematics of this phenomenon. Importantly, the general

observations are out of line with the intuitive expectation that smaller crystals are more likely to jump, as would be expected from their lower inertia. Instead, we found that there are optimal lengths of all crystal axes ( $l_{opt} = 500\text{--}600 \mu\text{m}$ ,  $w_{opt} = 300\text{--}400 \mu\text{m}$ ,  $t_{opt} = 100\text{--}200 \mu\text{m}$ ) and optimum volume of the crystal ( $V_{cropy} = 20\text{--}30 \times 10^7 \mu\text{m}^3$ ) for which the TS effect is manifested in the form of some of the three most frequent

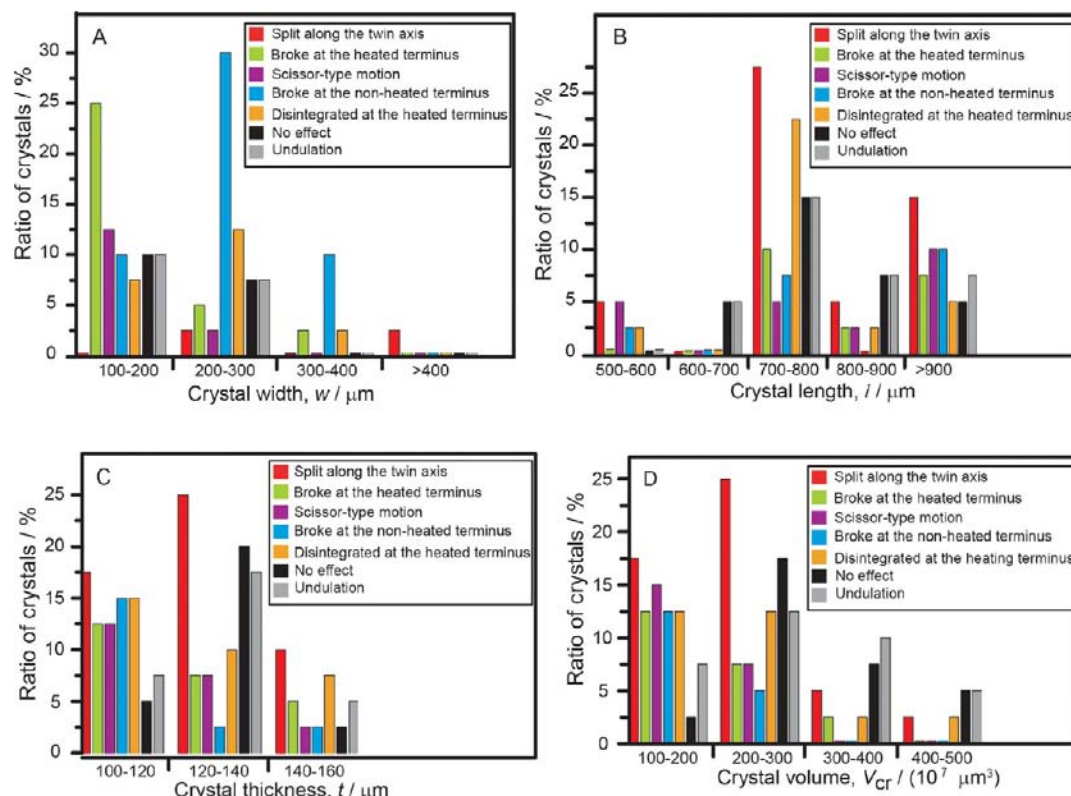


**Figure 6.** Distribution of the relative number of crystals over the kinematic effects for crystals heated locally and laterally ( $\perp l$ ) with respect to the longest axis. The number of crystals in a particular size range undergoing that effect was divided by the total number of crystals in the same range.

kinematic effects. Notably, in the case of the two shorter (width and thickness), medium-size crystals are most likely to jump. With respect to the length of the longest crystal axis, the shortest crystals are most easily actuated. With respect to the volume, it is less likely that the small crystals will jump, and the probability decreases with size. The maximum in the crystal distribution over the size appears to reflect two opposing contributions to the kinematics. The effect of the internal strain required for actuation of the crystal increases with the crystal size; the larger the crystal, the stronger the strain that can be accumulated in its interior. This effect is counter-balanced by the inertia which depends on the crystal mass; heavier crystals are less likely to jump relative to smaller crystals because of the larger energy required for their displacement. It should be also noted that for small, fast objects the drag forces are considerable and are expected to contribute significantly to the overall effect.

Since the direction of heating and the distribution of kinetic energy throughout a nonisotropic and heterogeneous body (twin) such as crystals of TBB are expected to have a profound effect on the thermomechanical effect, we also studied the effect of lateral heating ( $\perp l$ ) on the crystals. AC current was passed through a thin metal wire mounted on an XYZ micro-manipulator stage, and the heater was positioned close to and normal to the longest axis of the crystal that was affixed at one of its termini to a glass rod. This setup provided easy and controlled access and local exposure of the crystal to heat from different orientations during desired periods.

As anticipated, we observed a dramatically different kinematic behavior of the crystals and different distribution of the effects with respect to their size (Figure 6). Crystal explosion and jumping were less frequently observed, as would be

expected from the fact that one terminus of the crystal was affixed and the heating was localized. Correspondingly, the trends in the distribution of the effects over crystal size were much less obvious relative to the case of uniformly heated crystals.

However, in response to the forward and reverse phase transitions, periodic and alternating heating and cooling of the free terminus of such supported crystals caused reversible oscillations in the length of the heated crystal component. In effect, the periodic strain induced by the lattice dissimilarity between the transformed and nontransformed crystal component at the twinning face appeared as visible undulations that progressed along the longest axis of the crystal.<sup>78</sup> This deformation of the twinned crystal resembles bending of a bimetallic strip, with the different crystal orientation of the two components of the twin taking the role analogous to that of two different metals in a bimetallic strip. We found that, if the heating is retained at a moderate level and the temperature variation is maintained within certain limits close to the temperature of the phase transition (46 °C), this motion of the twin can be repeated indefinitely without any apparent crystal deterioration. The reversible motion of the two components in such an analogue of a bimetallic strip provides a rare example of reversible control over the thermomechanical motion of a crystal twin of purely organic material. This thermal control of the crystal actuation is possible due to the combination of crystal dynamics driven by the reversible, mechanically active phase transition, and the restoring action brought about by the cohesive force of the two crystal components.

At higher temperatures, in response to strong localized heating, we observed separation of debris from one or, less frequently, from both twinned components. At even higher

temperatures, by inducing phase transition in only one of the components of the twin, the crystal splits smoothly along the twinning interface. The separation of the twin occurs when the structural misfit between the two crystals over the twinned interface outweighs the binding energy (the collective intermolecular interactions) between the two components. The heated component expands along the longest axis relative to the nonheated one, causing the latter to deflect as a result of the strain that has evolved from the lattice misfit at the joint face. In effect, the two partially separated components can perform reversible scissor-like motion where they are periodically separated and rejoined (Figure 4D).

### 3. CONCLUSIONS

TBB is unique among the known TS materials in being the only compound that crystallizes as large, naturally twinned crystals. This extremely rare combination of properties (TS effect and twinning) sets the TBB crystals as an organic equivalent to a bimetallic strip, where the two components which are physically joined can respond to heating individually. With the TS transition close to ambient temperature, which is important for the envisaged practical applications, and having the structures of both phases related by the TS transition, TBB is an ideal structure to establish correlations between the atomic-level mechanistic details of the thermosalient effect and its macroscopic manifestation. Here, we have used TBB to assess, both at macroscale and at nanoscale, the effect of the mechanical properties of crystals that are capable of the TS effect on the mechanical response. The macroscopic response was analyzed through the kinematic analysis of the effect based on high-speed recordings of the jumping crystals.

The analysis revealed that the TS phenomenon is kinematically diverse and includes at least six types of effects. It occurs in two stages: during the first stage, strain is accumulated as a result of the phase transition, which is then suddenly released, resulting in a ballistic crystal displacement, oftentimes accompanied by separation of debris or explosion. These results complement the recent, more general considerations of the TS effect, where the underlying processes were considered analogous to the effects driving martensitic phase transitions in metal alloys.<sup>78</sup> The relative contribution of these two different kinematic effects depends on the size of crystals and the heating mode. The results from the mechanical characterization of the crystals are in strong support of this two-stage mechanism. We found that although macroscopically the TBB crystals are brittle entities, at the nanoscale they are unusually elastic. This elasticity appears to be a critical factor for accrual of strain without immediate structural reorganization (i.e., phase transition). Indeed, the TBB crystals remain susceptible to a significant amount of strain without response up to the point when the collective transformation of the molecular packing is triggered. A very rapid, nearly instantaneous structural transformation follows, which results in phase transition of domains and the entire crystal. The progression of this lattice deformation throughout the crystal in a preferred direction causes the crystal to move off the base. This process is oftentimes related to separation of debris from the crystal termini or with partial or complete disintegration. The brittleness observed in the macroscopic tests is in line with this consequence. The collective results presented here also have predictive power and point out the nanoscale elasticity of the crystals as one of the prerequisites for occurrence of the TS effect during a structural phase transition.

## 4. EXPERIMENTAL SECTION

**4.1. Preparation of the Crystals.** 1,2,4,5-Tetrabromobenzene (TBB) was obtained from Aldrich and recrystallized twice from toluene. Large crystals of centimeter size were harvested from an incubated toluene solution (60 °C) after a day. Regular, but smaller crystals are obtained by slow evaporation at ambient temperature. Microscopy under polarized light shows >95% twins.

**4.2. Nanoindentation.** The nanoindentation measurements were performed on the crystals using a nanoindenter (Triboindenter of Hysitron, Minneapolis, U.S.A.) with *in situ* AFM imaging capability. The machine monitors continuously and records the load,  $P$  and displacement,  $h$  of the diamond indenter during indentation with a force resolution of about 1 nN and a displacement resolution of about 0.2 nm. A Berkovich diamond tip with a tip radius of  $\sim 100$  nm was used for indentation. Residual indent impressions were captured immediately after unloading, to avoid time-dependent elastic recovery of the residual indent impression. The load was increased and decreased in a linear fashion (5 s load–2 s hold–5 s unload). Indents were made at constant load of 500–2500  $\mu\text{N}$  to measure mechanical properties, and a few were at 5 mN to capture residual indent impressions. Each test was performed at different positions on the sample for a minimum number of 17, and data were taken from the average of them. The  $P$ – $h$  curves were analyzed using the standard Oliver–Pharr method<sup>76</sup> to extract the  $H$  and  $E_r$  values of the crystals. More details on this method can be found elsewhere.<sup>77</sup>

**4.3. Kinematic Analysis.** The kinematic (motion) analysis was performed on well-shaped rod crystals of TBB and heated in two different modes, parallel ( $\parallel$ ) and perpendicular to the longest sides ( $\perp$ ). A total of 150 crystals were individually heated and examined with an ordinary digital camera or by using a high-speed camera. Both cameras were coupled to a reflectivity-mode optical microscope equipped with either a hot plate or a pointy heater. For recording the trajectory mode ( $\parallel$ ), the needle crystals were placed on a hot plate parallel to the longest crystallographic axis, and the maximum temperature was set close to 46–48 °C. During the trajectory mode ( $\perp$ ) every crystal was glued on one end with a solid support, and the other end was heated with a heater located closer to the crystal with the temperature close to 46–48 °C. For recording the fast motions, a high-speed camera with a resolution of up to  $10^4$  s<sup>-1</sup> was used.

## ■ ASSOCIATED CONTENT

### 📄 Supporting Information

Table with the crystal metrics (Table S1), microscopic images of the macroscopic mechanical tests (Figure S1), AFM image of the indented sample (Figure S2), and movies showing the thermosalient effect of TBB crystals (files si\_002.avi–si\_016.avi). This material is available free of charge via the Internet at <http://pubs.acs.org>.

## ■ AUTHOR INFORMATION

### Corresponding Author

P.N.: e-mail, [pance.naumov@nyu.edu](mailto:pance.naumov@nyu.edu); tel, +971-2-6284572.  
C.M.R.: e-mail, [cmallareddy@gmail.com](mailto:cmallareddy@gmail.com); tel, +913-3-25873118.

### Author Contributions

<sup>†</sup>S.C.S. and S.B.S. have contributed equally to this study.

### Notes

The authors declare no competing financial interest.

## ■ ACKNOWLEDGMENTS

This work was supported by funding from the NYU Abu Dhabi.

## ■ REFERENCES

- (1) Balzani, V. V.; Credi, A.; Raymo, F. M.; Stoddart, J. F. *Angew. Chem., Int. Ed.* **2000**, *39*, 3348.
- (2) Browne, W. R.; Feringa, B. L. *Nat. Nanotechnol.* **2006**, *1*, 25.

- (3) Kay, E. R.; Leigh, D. A.; Zerbetto, F. *Angew. Chem., Int. Ed.* **2007**, *46*, 72.
- (4) Jiménez, M. C.; Dietrich-Buchecker, C.; Sauvage, J.-P. *Angew. Chem., Int. Ed.* **2000**, *39*, 3284.
- (5) Liu, Y.; Flood, A. H.; Bonvallet, P. A.; Vignon, S. A.; Northrop, B. H.; Tseng, H.-R.; Jeppesen, J. O.; Huang, T. J.; Brough, B.; Baller, M.; Magonov, S.; Solares, S. D.; Goddard, W. A.; Ho, C.-M.; Stoddart, J. F. *J. Am. Chem. Soc.* **2005**, *127*, 9745.
- (6) Fletcher, S. P.; Dumur, F.; Pollard, M. M.; Feringa, B. L. *Science* **2005**, *310*, 80.
- (7) Garcia-Garibay, M. A. *Proc. Natl. Acad. Sci. U.S.A.* **2005**, *102*, 10771.
- (8) Behl, M.; Lendlein, A. *Soft Matter* **2007**, *3*, 58.
- (9) Lee, K. M.; White, T. J. *Macromolecules* **2012**, *45*, 7163.
- (10) Lee, K. M.; Koerner, H.; Wang, D. H.; Tan, L.-S.; White, T. J.; Vaia, R. A. *Macromolecules* **2012**, *45*, 7527.
- (11) Yu, Y.; Nakano, M.; Ikeda, T. *Nature* **2003**, *425*, 145.
- (12) Wu, W.; Yao, L.; Yang, T.; Yin, R.; Li, F.; Yu, Y. *J. Am. Chem. Soc.* **2011**, *133*, 15810.
- (13) Yu, Y.; Maeda, T.; Mamiya, J.-i.; Ikeda, T. *Angew. Chem., Int. Ed.* **2007**, *46*, 881.
- (14) Singleton, T. A.; Ramsay, K. S.; Barsan, M. M.; Butler, I. S.; Barrett, C. J. *J. Phys. Chem. B* **2012**, *116*, 9860.
- (15) Lendlein, A.; Jiang, H.; Jünger, O.; Langer, R. *Nature* **2005**, *434*, 879.
- (16) Camacho-Lopez, M.; Finkelmann, H.; Palffy-Muhoray, P.; Shelley, M. *Nat. Mater.* **2004**, *4*, 307.
- (17) Ahir, S. V.; Terentjev, E. M. *Nat. Mater.* **2005**, *4*, 491.
- (18) Welker, D. J.; Kuzyk, M. G. *Appl. Phys. Lett.* **1994**, *64*, 809.
- (19) Hrozhyk, U.; Serak, S.; Tabiryian, N.; White, T. J.; Bunning, T. J. *Opt. Express* **2009**, *17*, 716.
- (20) Lee, K. M.; Koerner, H.; Vaia, R. A.; Bunning, T. J.; White, T. J. *Macromolecules* **2010**, *43*, 8185.
- (21) Lee, K. M.; White, T. J. *Polymers* **2011**, *3*, 1447.
- (22) Wang, D. H.; Lee, K. M.; Yu, Z.; Koerner, H.; Vaia, R. A.; White, T. J.; Tan, L.-S. *Macromolecules* **2011**, *44*, 3840.
- (23) Lee, K. M.; Wang, D. H.; Koerner, H.; Vaia, R. A.; Tan, L.-S.; White, T. J. *Angew. Chem., Int. Ed.* **2012**, *51*, 4117.
- (24) Welker, D. J.; Kuzyk, M. G. *Appl. Phys. Lett.* **1995**, *66*, 2792.
- (25) Rochon, P.; Batalla, E.; Natansohn, A. *Appl. Phys. Lett.* **1995**, *66*, 136.
- (26) John, G.; Jadhav, S. R.; Menon, V. M.; John, V. T. *Angew. Chem., Int. Ed.* **2012**, *51*, 1760.
- (27) Cui, Q. H.; Zhao, Y. S.; Yao, J. J. *Mater. Chem.* **2012**, *22*, 4136.
- (28) Facchetti, A. *Chem. Mater.* **2011**, *23*, 733.
- (29) Fratzl, P.; Barth, F. G. *Nature* **2009**, *462*, 442.
- (30) Lv, S.; Dudek, D. M.; Cao, Y.; Balamurali, M. M.; Gosline, J.; Li, H. *Nature* **2010**, *465*, 69.
- (31) Reddy, C. M.; Krishna, G. R.; Ghosh, S. *CrystEngComm* **2010**, *12*, 2296.
- (32) Ghosh, S.; Reddy, C. M. *Angew. Chem., Int. Ed.* **2012**, *51*, 10319.
- (33) Kobatake, S.; Takami, S.; Muto, H.; Ishikawa, T.; Irie, M. *Nature* **2007**, *446*, 778.
- (34) Irie, M.; Kobatake, S.; Horichi, M. *Science* **2001**, *291*, 1769.
- (35) Al-Kaysi, R. O.; Müller, A. M.; Bardeen, C. J. *J. Am. Chem. Soc.* **2006**, *128*, 15938.
- (36) Terao, F.; Morimoto, M.; Irie, M. *Angew. Chem., Int. Ed.* **2012**, *51*, 901.
- (37) Bushuyev, O. S.; Singleton, T. A.; Barrett, C. J. *Adv. Mater.* **2013**, *25*, 1796.
- (38) Kim, T.; Zhu, L.; Mueller, L. J.; Bardeen, C. J. *CrystEngComm* **2012**, *14*, 7792.
- (39) Zhu, L.; Agarwal, A.; Lai, J.; Al-Kaysi, R. O.; Tham, F. S.; Ghaddar, T.; Mueller, L.; Bardeen, C. J. *J. Mater. Chem.* **2011**, *21*, 6258.
- (40) Good, J. T.; Burdett, J. J.; Bardeen, C. J. *Small* **2009**, *5*, 2902.
- (41) Koshima, H.; Ojima, N.; Uchimoto, H. *J. Am. Chem. Soc.* **2009**, *131*, 6890.
- (42) Koshima, H.; Ojima, N. *Dyes Pigments* **2012**, *92*, 798.
- (43) Koshima, H.; Takechi, K.; Uchimoto, H.; Shiro, M.; Hashizume, D. *Chem. Commun.* **2011**, *47*, 11423.
- (44) Boldyreva, E. V. *Mol. Cryst. Liq. Cryst.* **1994**, *242*, 17.
- (45) Boldyreva, E. V.; Sidel'nikov, A. A.; Chupakhin, A. P.; Lyakhov, N. Z.; Boldyrev, V. V. *Proc. Acad. Sci. USSR* **1984**, *277*, 893.
- (46) Boldyreva, E. V.; Sidel'nikov, A. A. *Proc. Sib. Dept. Acad. Sci. USSR* **1987**, *5*, 139.
- (47) Jakobson, B. I.; Boldyreva, E. V.; Sidel'nikov, A. A. *Proc. Sib. Dept. Acad. Sci. USSR* **1989**, *51*, 6.
- (48) Boldyreva, E. V.; Naumov, D. Yu.; Ahsbahs, H. *Acta Crystallogr., Sect. B* **1998**, *54*, 798.
- (49) Boldyreva, E. V.; Kuz'mina, S. L.; Ahsbahs, H. *J. Struct. Chem.* **1998**, *39*, 424.
- (50) Boldyreva, E. V.; Kuz'mina, S. L.; Ahsbahs, H. *J. Struct. Chem.* **1998**, *39*, 934.
- (51) Lieberman, H. F.; Davey, R. J.; Newsham, D. M. T. *Chem. Mater.* **2000**, *12*, 490.
- (52) Gafner, G.; Herstein, F. H. *Acta Crystallogr.* **1960**, *13*, 706.
- (53) Gafner, G.; Herstein, F. H. *Acta Crystallogr.* **1964**, *17*, 982.
- (54) White, K. M.; Eckhardt, C. J. *J. Chem. Phys.* **1989**, *90*, 4709.
- (55) Dye, R. C.; Eckhardt, C. J. *J. Chem. Phys.* **1989**, *91*, 3624.
- (56) Steiner, T.; Hinrichs, W.; Gigg, R.; Saenger, W. *Z. Kristallogr.* **1988**, *182*, 252.
- (57) Steiner, T.; Hinrichs, W.; Saenger, W.; Gigg, R. *Acta Crystallogr.* **1993**, *B49*, 708.
- (58) Kohne, B.; Praefcke, K.; Mann, G. *Chimia* **1988**, *42*, 139.
- (59) Fattah, J.; Twyman, J. M.; Dobson, C. M. *Magn. Reson. Chem.* **1992**, *30*, 606.
- (60) Zamir, S.; Bernstein, J.; Greenwood, D. J. *Mol. Cryst. Liq. Cryst.* **1994**, *242*, 193.
- (61) Skoko, Z.; Zamir, S.; Naumov, P.; Bernstein, J. *J. Am. Chem. Soc.* **2010**, *132*, 14191.
- (62) Ding, J.; Herbst, R.; Praefcke, K.; Kohne, B.; Saenger, W. *Acta Crystallogr.* **1991**, *B47*, 739.
- (63) Corbett, J. M.; Dickman, M. H. *Acta Crystallogr.* **1996**, *C52*, 1851.
- (64) Takemura, H. *Chemistry* **2005**, *60*, 46.
- (65) Crottaz, O.; Kubel, F.; Schmid, H. *J. Mater. Chem.* **1997**, *7*, 143.
- (66) Hirshfeld, F. L. *Theor. Chim. Acta* **1977**, *44*, 129.
- (67) McKinnon, J. J.; Spackman, M. A. *Chem. Commun.* **2007**, 3814.
- (68) McKinnon, J. J.; Mitchell, A. S.; Spackman, M. A. *Chem. Eur. J.* **1998**, *4*, 2136.
- (69) McKinnon, J. J.; Spackman, M. A.; Mitchell, A. S. *Acta Crystallogr.* **2004**, *B60*, 627.
- (70) Wolff, S. K.; Grimwood, D. J.; McKinnon, J. J.; Jayatilaka, D.; Spackman, M. A. *Crystal Explorer*; University of Western Australia: Perth, Australia, 2007.
- (71) Varughese, S.; Kiran, M. S. R. N.; Ramamurty, U.; Desiraju, G. R. *Angew. Chem., Int. Ed.* **2013**, *52*, 2701.
- (72) Kiran, M. S. R. N.; Varughese, S.; Reddy, C. M.; Ramamurty, U.; Desiraju, G. R. *Cryst. Growth Des.* **2010**, *10*, 4650.
- (73) Varughese, S.; Kiran, M. S. R. N.; Solanko, K. A.; Bond, A. D.; Ramamurty, U.; Desiraju, G. R. *Chem. Sci.* **2011**, *2*, 2236.
- (74) Kiran, M. S. R. N.; Varughese, S.; Ramamurty, U.; Desiraju, G. R. *CrystEngComm* **2012**, *14*, 2489.
- (75) Varughese, S.; Kiran, M. S. R. N.; Ramamurty, U.; Desiraju, G. R. *Chem.-Asian J.* **2012**, *7*, 2118.
- (76) Oliver, W. C.; Pharr, G. M. *J. Mater. Res.* **1992**, *7*, 1564.
- (77) Li, W.; Barton, P. T.; Kiran, M. S. R. N.; Burwood, R. P.; Ramamurty, U.; Cheetham, A. K. *Chem.-Eur. J.* **2011**, *17*, 12429.
- (78) Sahoo, S. C.; Panda, M.; Nath, N. K.; Naumov, P. Submitted for publication.